

Supporting Information Appendix for *In vitro* selection of a sodium-specific DNzyme and its application in intracellular sensing

Seyed-Fakhreddin Torabi^a, Peiwen Wu^a, Claire E. McGhee^b, Lu Chen^a, Kevin Hwang^b, Nan Zheng^c,
Jianjun Cheng^c, and Yi Lu^{a,b,c,1}

^a Department of Biochemistry, ^b Department of Chemistry, ^c Department of Materials Science and Engineering,
University of Illinois at Urbana-Champaign, Urbana, Illinois 61801, United States

¹To whom correspondence may be addressed. E-mail: yi-lu@illinois.edu

Contents

Section S1. Materials

Section S2. Experimental procedures

Section S3. SI Figures for *in vitro* selection of Na⁺-specific DNzyme

Section S4. SI Figures for design and development of DNzyme based sensors

Section S5. SI Figures for activity test of the intracellular sensor in buffer

Section S6. SI Figures for cell culture, sensor delivery and co-localization study

Section S7. SI Figures for live cell sodium imaging

Section S8. SI Tables

Section S9. SI References

Section S1. Materials

Chemicals: All oligonucleotides were purchased from Integrated DNA Technology Inc. (IDT) and purified by denaturing (8 M urea) 10 % polyacrylamide gel electrophoresis (PAGE) before use. Sensor oligonucleotides were synthesized and HPLC-purified by IDT. Details of the nucleotide sequences are provided in Sequences section. Other metal salts used included the following: LiCl.H₂O (Alfa Aesar, 99.996%), NaCl (Alfa Aesar, 99.999%), KCl (Alfa Aesar, 99.995%), RbCl (Alfa Aesar, 99.975%), CsCl (Alfa Aesar, 99.999%), NH₄CH₃CO₂ (Aldrich, 99.999%), MgCl₂.6H₂O (Alfa Aesar, 99.999%), Ca(NO₃)₂.6H₂O (Alfa Aesar, 99.995%), SrCl₂.6H₂O (Alfa Aesar, 99.996%), BaCl₂.2H₂O (Alfa Aesar, 99.997%), Mn(CH₃CO₂)₂.4H₂O (Alfa Aesar, 99.999%), CoCl₂.6H₂O (Alfa Aesar, 99.9%), NiCl₂.6H₂O (Alfa Aesar, 99.995%), Cu(NO₃)₂.H₂O (Alfa Aesar, 99.999%), ZnCl₂.H₂O (Alfa Aesar, 99.99%), Cd(NO₃)₂.4H₂O (Alfa Aesar, 99.999%), HgCl₂ (Alfa Aesar, 99.999%), Pb(CH₃CO₂)₂.3H₂O (Aldrich, 99.999%), InCl₃ (Aldrich, 99.999%), La(NO₃)₃.6H₂O (Aldrich, 99.999%), EuCl₃.6H₂O (Aldrich, 99.999%), SmCl₃.6H₂O (Aldrich, 99.99%), and YbCl₃.6H₂O (Aldrich, 99.998%). Salts and solutions used to adjust pH of buffer solutions included the following: LiOH.H₂O (Alfa Aesar, 99.996%) NaOH.H₂O (Alfa Aesar, 99.996%), KOH (Fisher Scientific), and 36.5% HCl (Alfa Aesar, 99.999%). Other chemicals used to prepare different solutions included the following: Ethylenediaminetetraacetic acid, sodium free (EDTA) (Fluka, 99.0%), EDTA.2Na.2H₂O (Fisher Scientific), Trisodium citrate (Alfa Aesar, 99%), urea (Affymetrix, MB grade), Tris (Affymetrix, MB grade), boric acid (Fisher Scientific, electrophoresis grade), and Bis-Tris (Sigma, 99.0%). Acrylamide/bisacrylamide 40% solution (29:1) was obtained from Bio-Rad. *Taq* DNA polymerase with standard *Taq* buffer, T4-polynucleotide kinase, and deoxynucleotide (dNTP) solution mix were obtained from New England Biolabs. ³²P labeled α-ATP and γ-ATP for DNA radiolabeling was obtained from Perkin-Elmer. All buffer, metal ion and gel stock solutions were prepared with Milli-Q water. The pH of the buffers was measured with Fisher Scientific Accumet AB15 pH meter.

Sequences: 1. Template and primers used in selection:

DNA Template: 5'-GGAAGTACCGCATGGTAC-N₅₀-CGTGAGCCTACGATGAGAC-3'

P1: 5'-GTCTCATCGTAGGCTCAC-3' (PCR1 and 2)

P2: 5'-GACTAATTCATCACGTATAGGAAGTACCGCATG-3' (PCR1)

P3: 5'-Biotin-GTTCAGACTAATCATCACGTATrA-3' (PCR2)

P4: 5'-GACAACAACAACAAC(internal spacer-C18)GTCTCATCGTAGGCTCAC-3' (PCR1 and 2)

P5: 5'-GTTCAGACTAATCATCACGTATrA-3' (PCR2)

NaA43 trans-cleaving form with four different binding arms as represented in *SI Appendix*, Fig. S9.

NaA43S #1: 5'-GGATCACGTATrAGGAAGTACCGCC-3'

NaA43E #1: 5'-GGCGGTACCAGGTCAAAGGTGGGTGAGGGGACGCCAAGAGTCCCCGCGGTTACGTGATCC-3'

NaA43S #2: 5'-CTCTATGTATrAGGAAGTACCGCCG-3'

NaA43E #2: 5'-GCGGCGGTACCAGGTCAAAGGTGGGTGAGGGGACGCCAAGAGTCCCCGCGGTTACATAGAG-3'

NaA43S #3: 5'-ACTCACTATrAGGAAGAGATGGACGTG-3'

NaA43E #3: 5'-CACGTCCATCTCCAGGTCAAAGGTGGGTGAGGGGACGCCAAGAGTCCCCGCGGTTAGTGAGT-3'

NaA43S #4: 5'-GGATGTATrAGGAAGTACCGCC-3'

NaA43E #4: 5'-GGCGGTACCAGGTCAAAGGTGGGTGAGGGGACGCCAAGAGTCCCCGCGGTTACATCC-3'

2. Fluorescence sensors:

NaA43S FAM/IABkFQ: 5'-/6-FAM/CTCTATCTATrAGGAAGTACCGCCG/IABkFQ/-3'

NaA43E IABkFQ: 5'-
GCGGCGGTACCAGGTCAAAGGTGGGTGAGGGGACGCCAAGAGTCCCCGCGGTTAGATAGAG/IABkFQ/-3'

3. Co-localization study:

FAM-dANa43S: 5' -/6-FAM/ACTCACTATAGGAAGAGATGGACGTG-3'

Na43E: 5' -ACGTCCATCTCCAGGTCAAAGGTGGGTGAGGGGACGCCAAGAGTCCCCGCGGTTAGTGAG-3'

Na43E-Cy3: 5' -

A*C*GTCCATCTCCAGGTCAAAGGTGGGTGAGGGGACGCCAAGAGTCCCCGCGGTTAGTG*A*G/3Cy3ph/-3'

4. Intracellular sensing:

4.1 Active NaA43E with caged NaA43S/non-cleavable NaA43S

4.1.1 Positive group: Active NaA43E (IBQ) + Caged NaA43S (FAM-BHQ1)

Active NaA43E (IBQ): 5' -

A*C*GTCCATCTCCAGGTCAAAGGTGGGTGAGGGGACGCCAAGAGTCCCCGCGGTTAGTG*A*G/3IABkFQ/-3'

(* represents phosphorothioate modification)

Caged Na43S (FAM-BHQ1): 5' -/6-FAM/ACTCACTAT/iNiBenz-rA/GGAAGAGATGGACGTG/BHQ_1/-3'

4.1.2 Control: Active NaA43E (IBQ) + Non-cleavable NaA43S (FAM-BHQ1)

Active NaA43E (IBQ): 5' -A*C*GTCCATCTCCAGGTCAAAGGTGGGTGAGGGGACGCCAAGAGT-3'

Non-cleavable NaA43S (FAM-BHQ1): 5' -/6-FAM/ACTCACTATAGGAAGAGATGGACGTG/BHQ_1/-3'

4.2 Active NaA43E/Inactive NaA43E with caged NaA43S

4.2.1. Positive group: Active NaA43E (IBRQ) + Caged NaA43S (TAMRA-BHQ2)

Active NaA43E (IBRQ):

5' -A*C*GTCCATCTCCAGGTCAAAGGTGGGTGAGGGGACGCCAAGAGTCCCCGCGGTTAGTG*A*G/IABrQSp/-3'

Caged NaA43S (TAMRA-BHQ2): 5' -/6-TAMN/ACTCACTAT/iNiBenz-rA/GGAAGAGATGGACGTG/BHQ_2/-3'

4.2.2. Control: Inactive NaA43E (IBRQ) + Caged NaA43S (TAMRA-BHQ2)

Inactive NaA43E (IBRQ):

5' -A*C*GTCCATCTCCAGGTCAAAGGTGGGTGAGGGGACGCCAAGAGTCCCCGCGGTTAGTG*A*G/IABrQSp/-3'

Caged NaA43S (TAMRA-BHQ2): 5' -/6-TAMN/ACTCACTAT/iNiBenz-rA/GGAAGAGATGGACGTG/BHQ_2/-3'

Section S2. Experimental Procedures

In vitro selection: The same initial selection pool was used for both selections and was generated through template-directed extension followed by two PCR amplifications. For each selection, the extension reaction was carried out in two steps. In the first step, 300 pmol of DNA template and 300 pmol of primer P1 were mixed in 60 × 50 µl reaction mixtures and extended for two thermal cycles (1 min at 94°C, 1.5 min at 58°C and then 3 min at 72°C). Second step was carried out by addition of 450 pmol of primer P2 and two more thermal cycles. The reaction buffer also included 0.1 units/µl of Taq DNA polymerase (New England Biolabs (NEB)), 1.5 mM MgCl₂, 50 mM KCl, 10 mM Tris-HCl (pH 8.3 at 25°C), and 0.2 mM of each dNTP. After two-step extension, 150 pmol of P2 and 3 nmol of P1 were added to the mixture reaction for ten additional amplification cycles (PCR1). Next, second PCR amplification was carried out by addition of 3 nmol of P3 and ten more thermal cycles to incorporate the rA cleavage site into the PCR product. Amplification of the isolated DNA at the end of each selection round was carried out by two PCR reactions. In PCR1 isolated DNA was amplified with skewed ratio of P1 (1.0 µM) to P2 (0.1 µM). 10% of PCR1 reaction was used as template in PCR2 and amplified with skewed ratio of P3 (1.0 µM) to P1 (0.1 µM). PCR2 products were internally

labeled with [α - 32 P]-dATP (PerkinElmer) to keep track of DNA pools and cleavage products through selection process via liquid scintillation counting and denaturing PAGE analysis.

PCR amplified pools were immobilized on NeutrAvidin agarose beads using buffer A (10 mM Bis-Tris (pH 7.0 at 24 °C) and 1 mM EDTA) over 10 minutes (*SI Appendix*, Fig. S1). Single stranded DNA pools were generated by washing beads with buffer B (150 mM NaOH and 2 mM EDTA) at 45 °C for 1 min followed by three more washing steps with ice cold buffer B and then ice cold distilled water. Background cleavage was collected using buffer C (50 mM Bis-Tris (pH 7.0 at 24 °C) and 1 mM EDTA). Two parallel selections were carried out using two different sodium concentrations. In selection A active DNazymes were collected by incubating immobilized pool with a solution containing 50 mM Bis-Tris (pH=7.0 at 24 °C), 1 mM EDTA, 10 mM sodium citrate and 105 mM NaCl (total of ~135 mM Na⁺). Selection B was carried out using a solution containing 50 mM Bis-Tris (pH=7.0 at 24 °C), 1 mM EDTA, 10 mM sodium citrate and 370 mM NaCl (total of ~ 400 mM Na⁺). Selected DNA sequences were PAGE purified and used as PCR template to generate pools for the next round of the selection. As it is shown in *SI Appendix*, Fig. S2 PAGE purification was an important part of the selection to remove nonspecific detachment of uncleaved sequences from beads. The PAGE purification step was critical especially at early rounds of the selection (*SI Appendix*, Fig. S2), since nonspecific detachment of uncleaved DNA sequences from the beads was much higher than release of the active sequences upon cleavage reaction. In previous reports column-based selection was used to isolate divalent metal ion-dependent DNazymes (1-3). It is known that divalent metal ions, in general, are significantly more effective as cofactors in ribozyme/DNAzyme catalysis. Therefore, initial activity of the random pool in the presence of divalent metal ions might be higher than nonspecific detachment of uncleaved sequences. In contrast, in our case the only available metal cofactor was Na⁺, a monovalent metal ion. Therefore, having a high ratio of nonspecific detachment of uncleaved sequences over Na⁺-specific cleavage may be expected. As shown in *SI Appendix*, Fig. S2 nonspecific detachment was dominant in the first two rounds. Immobilized DNA pools were incubated with selection buffers for 2 h at the first and the second rounds of the selection and incubation time was reduced subsequently to 45 seconds at round 15. Amplification of selected pools for analysis of their activity were carried out by using P4 and P5 primers instead of P1 and P3, respectively. P4 contained a hexaethyleneglycol spacer which served as a DNA polymerization termination site, followed by 5' -GACAACAACAACAAC-3', which resulted in formation of two strands of unequal lengths as PCR products. Amplified DNA pools contained rA cleavage site were separated from the longer PCR product via denaturing PAGE and precipitated with ethanol. Selected pools from the last three rounds of selections were tested further to find the most active pools for cloning and sequencing experiments. Selected pools from round 13 and 15 were chosen for cloning for selection condition A and B, respectively. TA-TOPO Cloning Kit (Invitrogen) was used for cloning experiments. The vectors were transformed into E. coli competent cells through heat-shock and ampicillin resistant transformants were selected on ampicillin containing LB plates. From each selection total of 50 randomly chosen colonies were grown in 5 ml LB culture with 100 μ g ml⁻¹ ampicillin at 37°C. DNA was extracted using Miniprep Kits (QIAGEN) and eluted into water. All clones were submitted to the University of Illinois Sequencing Center. Sequence analysis and alignment were performed by Vector NTI Advance 11.0 (Invitrogen). Secondary structure of DNazymes were predicted using UNAFold and DINAMelt packages (4, 5).

Several methods were used to monitor selection progress and enrichment of the DNA pools with Na⁺-specific DNazymes. First, the fraction of the cleaved versus the initial population of the pool was calculated at each round of selection (via liquid scintillation counting and denaturing PAGE analysis) (*SI Appendix*, Fig. S3). Second, the signal to background ratio was measured at each round of the selection, by comparing the amount of cleavage that occurred in buffer without Na⁺, with the cleavage from each round of selection (*SI Appendix*, Fig. S4). Third, since the reaction time was shortened through increasing rounds of selection, to offer fair assessment of enriching the selection pool with Na⁺-DNazymes, a parallel experiment was conducted with a constant reaction time, beginning from the fourth round of the selection (*SI Appendix*, Fig. S5). Lastly, starting at round five, the activity of the selected pools was tested every other round at different Na⁺ concentrations and the apparent k_{obs} for the cleavage were plotted versus selection rounds (*SI Appendix*, Fig. S6).

To monitor selectivity of the pools for Na⁺, their activity was tested in the presence of other monovalent ions including Li⁺, K⁺, Rb⁺, Cs⁺, or NH₄⁺ at 500 mM, cobalt hexamine at 40 mM or Pb²⁺ at 1 mM. The cobalt hexamine was used as an inert metal complex and a divalent metal ion mimic (6), while the Pb²⁺-dependent activity was tested due to the commonly-observed persistence of the 8-17 DNAzyme motif, which shows fast reaction rate in the presence of Pb²⁺

(7). It has been shown that undesired cross-reactivity with other metal ions could be minimized through counter-selection to remove cross-reactive species (8, 9). Due to the absence of cross reactivity with competing metal ions in our systems, no counter-selection step was incorporated into the selections. Interestingly, the selection B pools had higher signal over background and more cleavage than the selection A pools (*SI Appendix*, Fig. S3-5), probably because the concentration of Na⁺ in selection B was ~ 3 times higher than in selection A. In contrast, selected pools from selection A have shown higher rates of cleavage at lower Na⁺ concentrations and better sensitivity (*SI Appendix*, Fig. S6).

In total, 48 clones from selection A and 47 clones from selection B were obtained from the selected population. On the basis of sequence similarities, the obtained clones from selection A and B could be classified into two and three major classes, respectively (*SI Appendix*, Table S1-2). The Class A-II members showed a high degree of sequence similarity to class B-I. The Class A-II and B-I shared a common consensus sequence in the 50 nucleotides random-region (*SI Appendix*, Table S3). After screening the activity of individual clones from different classes, we found that the DNAzyme with highest activity belongs to class A-II.

Activity Assay: Activities of selected pools and *cis*-cleavage form of the DNAzyme was tested in 50 mM Bis-Tris (pH 7.0) and the reaction was initiated by addition of Na⁺ at desired concentration. DNA sequences were internally labeled during PCR amplification with [α -³²P]-dATP (PerkinElmer). Selectivity of *trans*-cleavage form of NaA43 DNAzyme for Na⁺ over Cu²⁺ and Hg²⁺ was tested under single turn-over condition using final concentration of 2 μ M and 10 nM for the enzyme and substrate, respectively. The substrate was labeled at 5'-end with [γ -³²P]-ATP (PerkinElmer) using T4 polynucleotide kinase from NEB. The DNAzyme complex containing the NaA43E and ³²P-labeled NaA43S was denatured by heating the mixture at 90°C for 3 min and annealed in buffer C (50 mM Bis-Tris (pH 7.0) containing 90 mM LiCl) by gradual cooling to room temperature over 30 min. For all activity assay experiments, cleavage reactions were quenched by addition of 2 μ l of the reaction mixture to 30 μ l of a “stop solution” containing 9 M urea, 1 \times TBE and 0.05 % each bromophenol blue and xylene cyanol. We verified that using a large volume (15 \times) of stop solution with high concentration of a denaturing reagent such as urea which would dilute Na⁺ concentration significantly is an effective method to quench the DNAzyme reaction. Samples from the zero time points were mixed with the stop solution at the end of the activity assay to test the cleavage in the absence of Na⁺. The cleaved and uncleaved substrate were separated by 10% or 20% denaturing PAGE and gel images were taken by Molecular Dynamics Storm 430 phosphorimager (from Amersham Biosciences). Kinetic curves were plotted using OriginLab 9.1 and fit to the equation of %P_{cleavage,t} = %P_{max} (1 - e^{-kt}), where %P_{max} is the maximum percent of cleavage product at the end of the reaction and *k* is the rate of cleavage (10).

Preparation of Sensor and Na⁺ Detection: The enzyme-substrate complex was formed by annealing a mixture of NaA43E and NaA43S (1.2 to 1 ratio) in buffer C. Concentrated Na⁺ or other metal solutions in buffer C were mixed with annealed complex before recording fluorescence change. Final concentration of the sensor complex was calculated to be 50 nM. Fluorescence change was continuously monitored by a FluoroMax-2 fluorometer (Horiba Jobin Yvon, Inc., Edison, NJ) every 12 s for at least 15 min. The excitation wavelength was 490 nm and emission was monitored at 520 nm. The initial rate of fluorescence enhancement, attributed to the release of the cleaved substrate, was measured by plotting the change in fluorescence intensity for the first 2 min after addition of Na⁺ using a linear fit. Other metal salts used as in material section of supporting information. Selectivity of the sensor for Na⁺ over other metal ions was tested in the presence of 22 different metal salts. Sensor response to monovalent competing cations (Li⁺, K⁺, Rb⁺, Cs⁺, NH₄⁺) was tested at 100 mM, while divalent (Mg²⁺, Ca²⁺, Sr²⁺, Ba²⁺, Mn²⁺, Co²⁺, Ni²⁺, Cu²⁺, Zn²⁺, Cd²⁺, Hg²⁺, Pb²⁺) and trivalent (In³⁺, La³⁺, Eu³⁺, Sm³⁺, Yb³⁺) metal ions were tested at 2 mM and 0.2 mM, respectively. It is known that metal ions such as Cu²⁺ and Hg²⁺ induce a strong quenching on FAM (5), therefore the performance of the sensor with Cu²⁺ and Hg²⁺ was tested using a gel-based method. No cleavage was observed in response to either Cu²⁺ or Hg²⁺, while incubation with Na⁺ resulted in a significant increase in cleavage (*SI Appendix*, Fig. S12). Interference of other monovalent metal ions and certain divalent metal ions known to be abundant within cells was tested on sensor response to Na⁺. It is confirmed that the sensor works in the presence of competing monovalent metal ions without significant interference, as well as having similar activity in the presence of divalent metal ions at their intracellular concentrations (difference in the rate of fluorescence enhancement within less than 1 fold) (*SI Appendix*, Fig. S14).

Activity test of the intracellular sensor in buffer: Active NaA43E (IBRQ) and Caged NaA43S (TAMRA-BHQ2) were mixed in Buffer K at a final concentration of 10 μ M. The two strands were annealed by heating the solution to 75°C for 2 min followed by slowly cooling down to room temperature over 1h. To restore the activity of the caged substrate strand, the solution was added into one of the wells in a 12-well plate, and exposed to UV light from a hand lamp at 365 nm for 30 min. Buffer solutions with different concentrations of Na⁺ were prepared by mixing Buffer K with Buffer Na at different ratios. Buffer solutions were spiked with the sensor solution after the decaging process, and fluorescence change was monitored using a fluorometer (Jobin Yvon FluoroMax-P) at 541 nm excitation and 568 nm emission over a time period of 20 min.

Buffer K: 12.5 mM HEPES, 140 mM KCl, 10 mM Glucose, 1.2 mM MgCl₂, 1 mM CaCl₂, pH 7.4

Buffer Na: 12.5 mM HEPES, 140 mM NaCl, 10 mM Glucose, 1.2 mM MgCl₂, 1 mM CaCl₂, pH 7.4

Cell culture, sensor delivery and co-localization study: HeLa cells were cultured in Dulbecco's modification of Eagle's medium (DMEM) supplemented with 10% Fetal Bovine Serum (FBS), 100 U/mL penicillin, and 100 μ g/mL streptomycin, on 25 cm² culture flasks at 37°C in a humidified 5% CO₂ incubator. Before imaging, cells were plated in 35 mm glass-bottom dishes (MatTek) and grown to 70-90% confluence.

For the delivery of DNAzyme sensors using cationic helical polypeptide G8, the corresponding NaA43E and NaA43S (final concentration of 0.1 mM) were mixed in the buffer containing 20 mM MOPS, 100 mM NaCl with pH at 7.1. To anneal the DNAzyme for better hybridization, the mixture was heated to 75°C for 2 min and slowly cooled down to room temperature for 30 min. G8 polypeptide (degree of polymerization=50) was dissolved in water at 0.2 mg/ml and the pH of the solution was adjusted to 6 using diluted HCl for better solubility. 45 μ l of polypeptide G8 was mixed and incubated with 2 μ l of the aforementioned NaA43ES construct for another 30 min to allow the formation of polymer-DNA complex (G8-NaA43ES). Normal cell culture medium was replaced with OPTI-MEM before the G8-NaA43ES complex solution was added to the cells grown in the plates.

After incubating HeLa cells with G8-NaA43ES complex for 4 hours, cells were washed thoroughly with PBS to remove excess amount of G8-NaA43ES complex in the medium. Specific organelles inside cells were stained with commercial dyes, such as Hoechst 33258, LysoTracker Red DND-99, MitoTracker Red CMXRos, and ER tracker Red. Early endosomes were tracked by transfecting HeLa with the CellLight early endosomes-RFP protein overnight before adding G8-NaA43ES complexes. Early endosomes-RFP is a construct where RFP is fused to Rab5a, providing specific targeting to cellular early endosomes without being affected by organelle pH. Images were obtained using a Zeiss LSM 710 NLO confocal microscope at 63 \times magnification equipped with a Mai-Tai Ti-Sapphire laser. Fluorescence emission of Hoechst 33258 was measured over 450-520 nm ranges, with excitation at 401 nm. Fluorescence of early endosomes-RFP, LysoTracker, MitoTracker and ER tracker was obtained by exciting at 561 nm and measuring over 575-610, 575-620 nm, 585-630 nm, and 600-650 nm, respectively. The pinhole and gain settings were kept constant throughout the whole imaging process. Z-stack images were also obtained to confirm that the fluorescent signal was inside cells.

Intracellular sodium sensing: HeLa cells were cultured in glass bottom dishes until about 80% confluence. After treatment with corresponding NaA43ES construct for 4 hours, cells were washed thoroughly with DPBS. Then cells were immersed in DPBS and irradiated with UV lamp at 365 nm for 30 minutes. Immediately after UV treatment, stock solutions of gramicidin D, monensin and ouabain were added to the cells at final concentrations of 3 μ M, 10 μ M and 100 μ M, respectively. Fluorescent images as well as bright field images were taken every 5 minutes immediately after addition of the ionophores and the ATPase inhibitor.

Section S3. SI Figures for *in vitro* selection of a Na⁺-specific DNAzyme

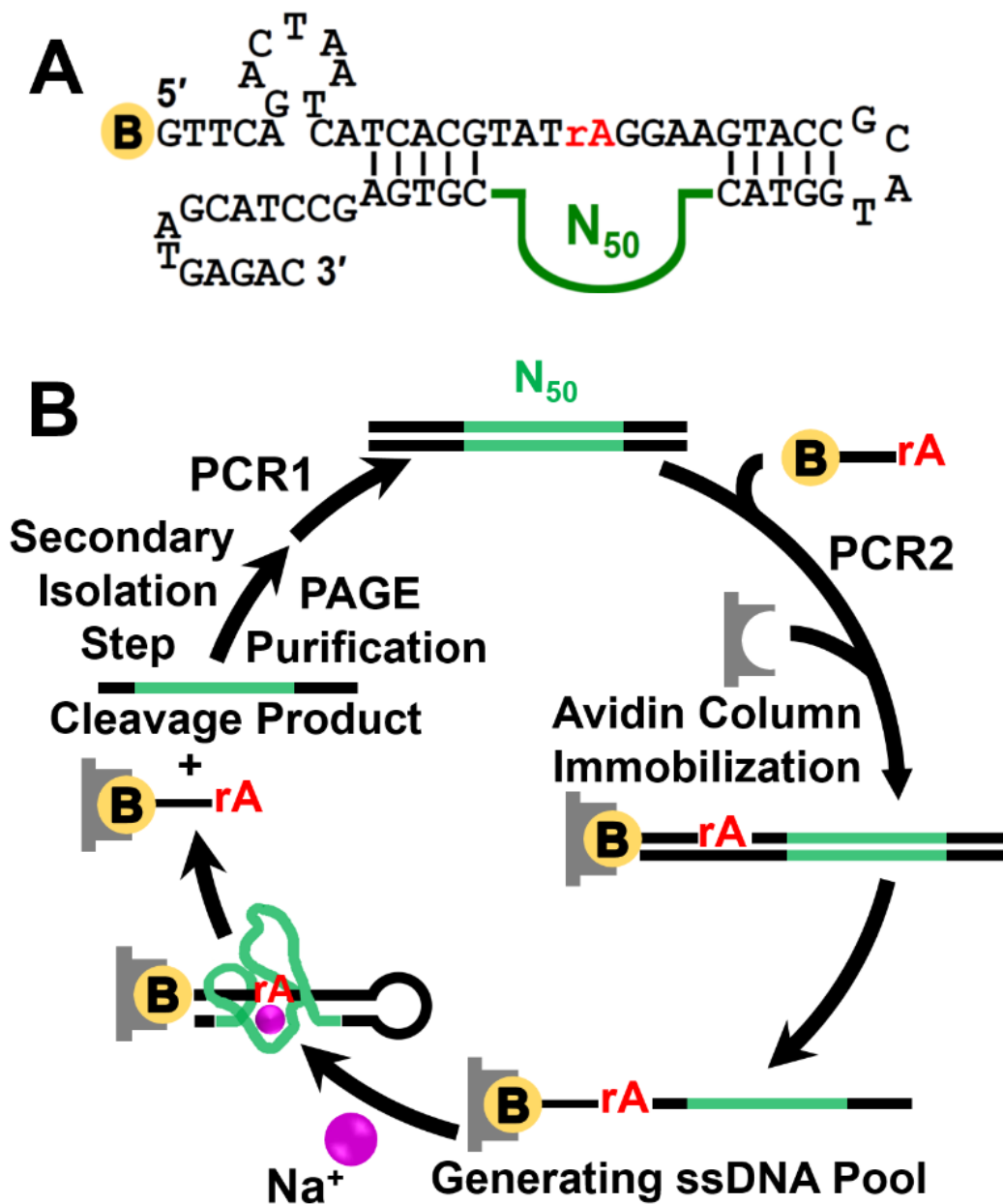


Figure S1. *In vitro* selection of a Na⁺-specific DNAzyme. (A) Design of the initial pool sequence. (B) Scheme of *in vitro* selection strategy. A PAGE purification step was incorporated into the selection protocol before PCR1 as a secondary isolation step to remove nonspecific detachment of uncleaved DNA from the column.

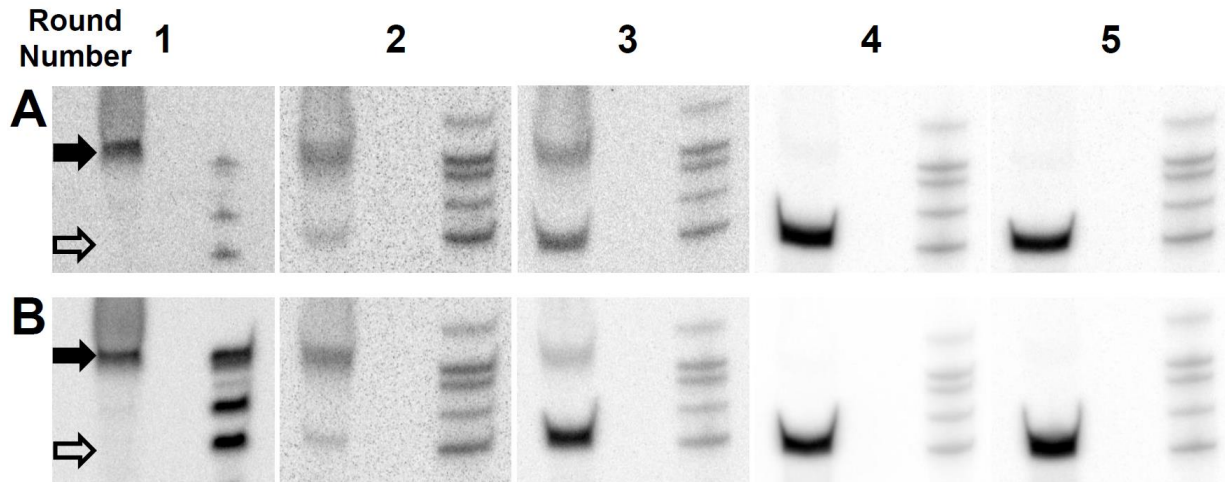


Figure S2. Secondary isolation step using denaturing PAGE purification. Gel images of eluted DNA from selection columns for the first five rounds of Na^+ -specific DNAzyme selection (A and B indicating selection A or B). Combining column-based selection method with PAGE purification guarantees isolation of only active sequences. In the first round of *in vitro* selection, active sequences (open arrows) eluted from selection columns were below the phosphorimaging detection limit, and only nonspecific detachment of uncleaved DNA was observed (filled arrows). From the second round of selections, cleavage products were detectable in phosphorimaged gels. Ratio of nonspecific detachment of DNA over active DNA cleavage increased significantly in the subsequent rounds. These results indicate that PAGE purification steps in our *in vitro* selection strategy are important to remove inactive sequences from eluted DNA at the end of each selection round and before amplification of active sequences.

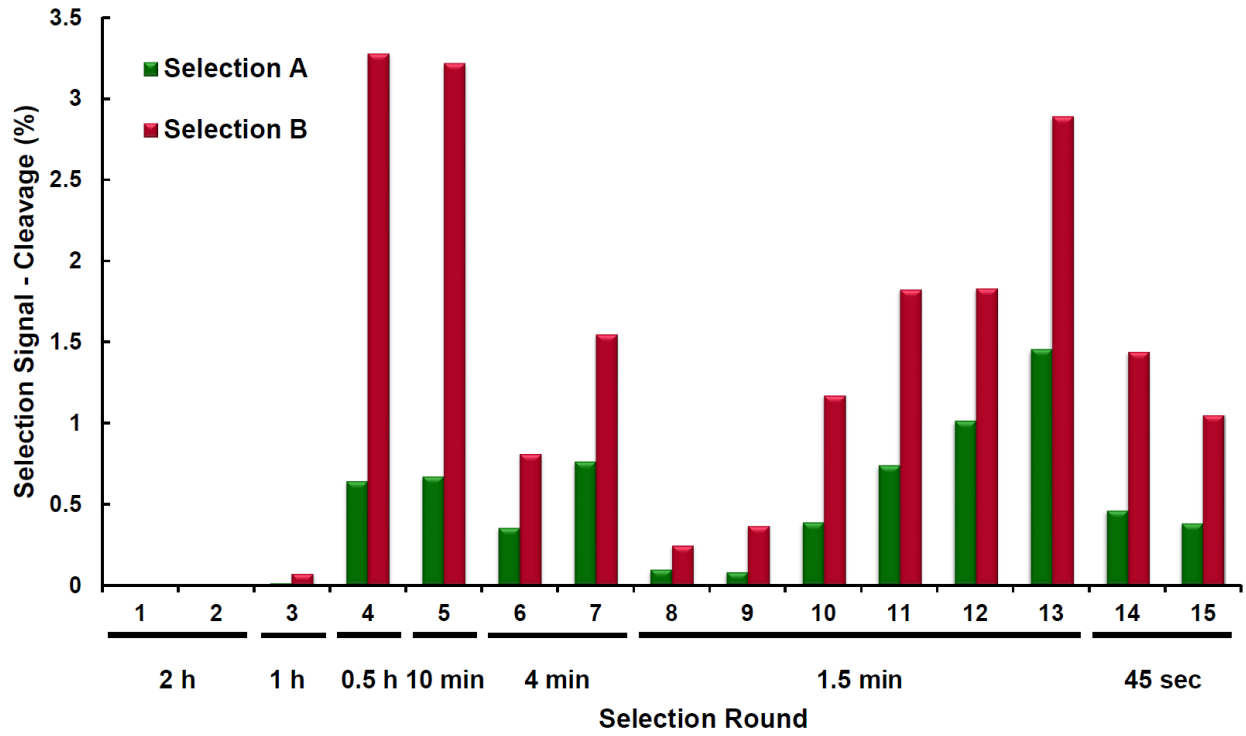


Figure S3. *In vitro* selection progress at each specific round represented in percentage fraction of cleaved DNA eluted off the column versus initial immobilized pool. Incubation time is displayed for each round.

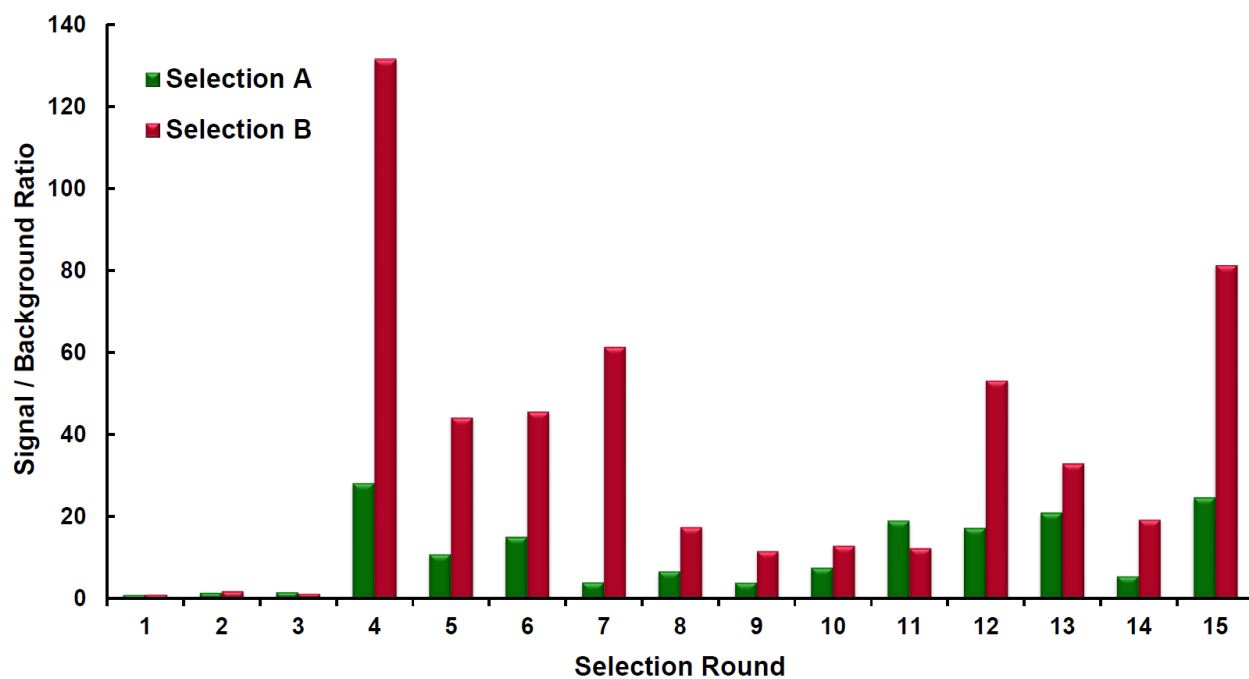


Figure S4. *In vitro* selection progress at each specific round represented as signal over background cleavage ratio. At each round, signal was the fraction of cleaved DNA in the presence of Na^+ , and background was the fraction of cleaved DNA in the absence of Na^+ .

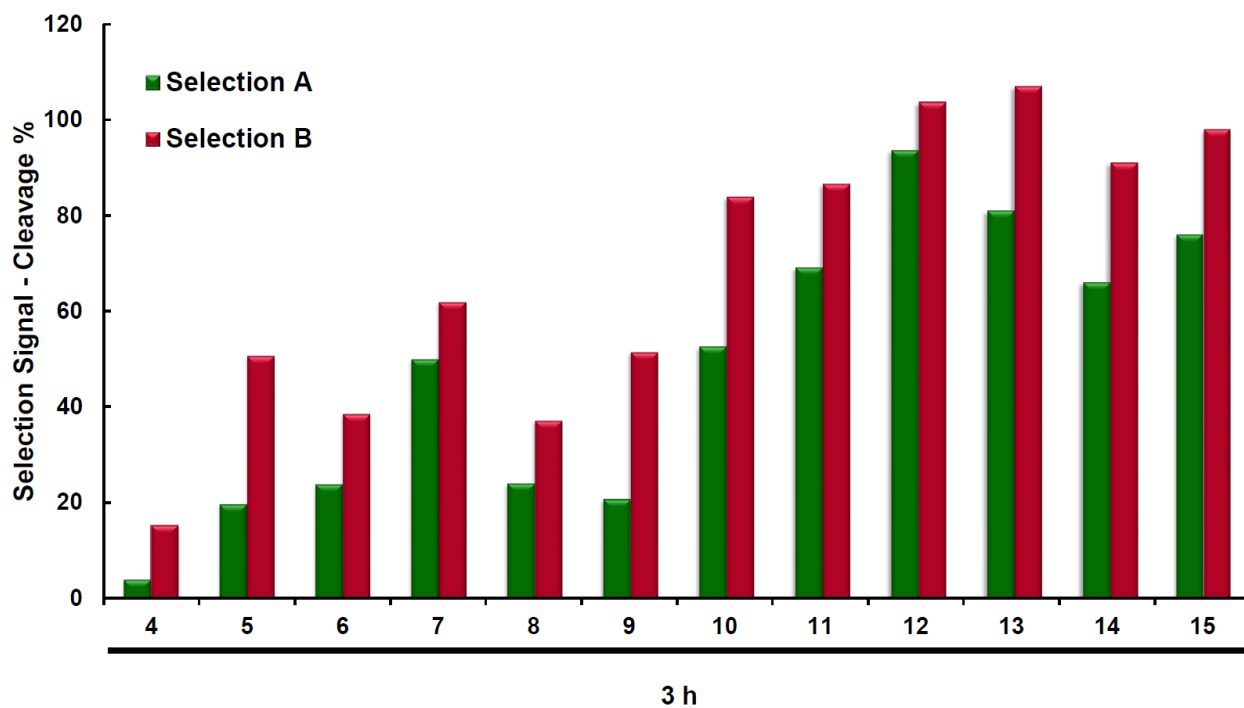


Figure S5. *In vitro* selection progress monitored from round 4 by determining percentage fraction of cleaved DNA eluted off the column versus initial immobilized pool over the course of three hours incubation with Na⁺ in selection buffer.

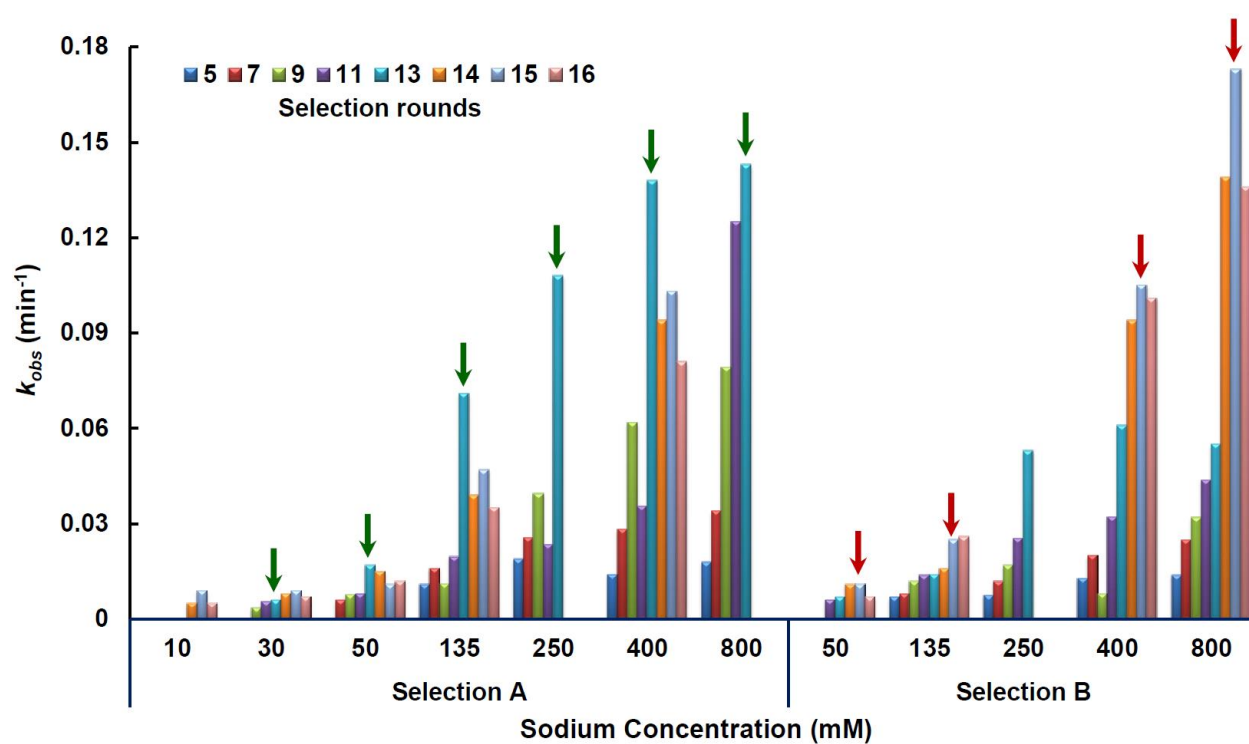


Figure S6. *In vitro* selection progress is followed from round 5 by calculating the observed apparent rate constants (k_{obs}) of selected pools at different Na^+ concentrations. Specific pools from selection A and B showing overall highest activities are marked by arrows.

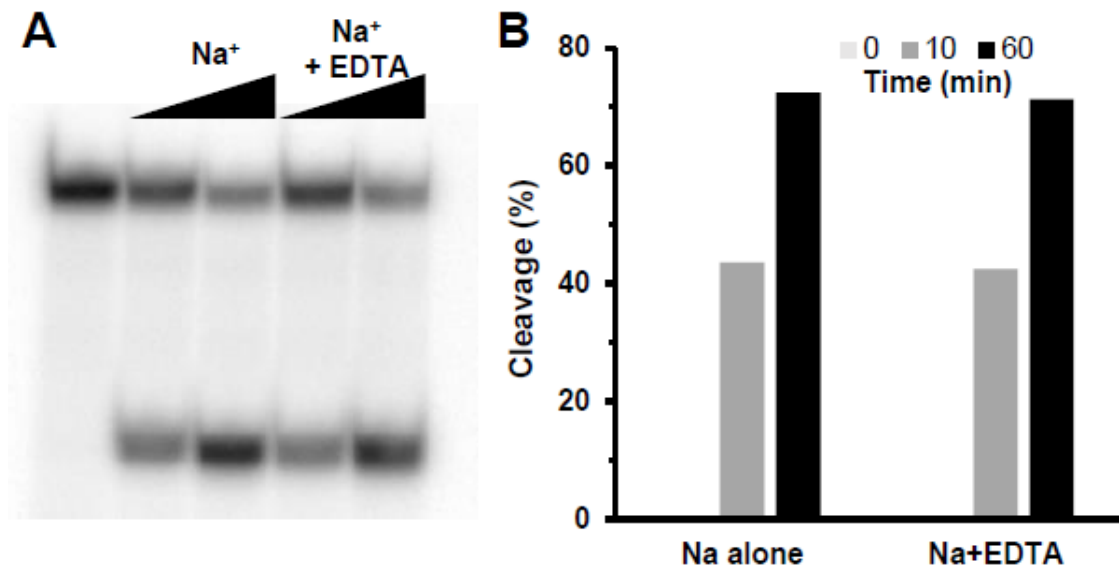


Figure S7. (A) Gel image of NaA43 DNase activity assay after incubation with 100 mM Na⁺ in the presence or absence of 50 mM EDTA. First lane is before addition of Na⁺. (B) Quantification of the gel data in A.

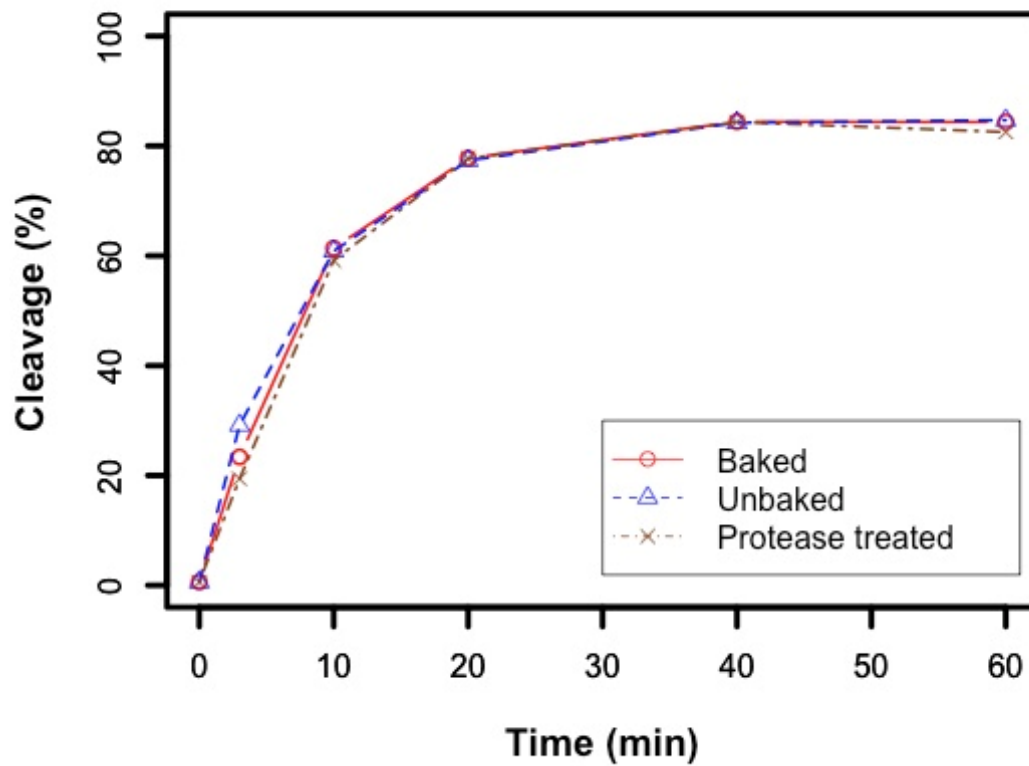


Figure S8. Activity of NaA43 DNAzyme in the presence of 400 mM of NaCl from different Na salt sources. Red line with circle - using NaCl baked at 260 °C for 36 hours; Blue line with triangle - using unbaked NaCl; Brown line with cross mark - using NaCl stock solution pre-treated with proteinase K at 37 °C for 24 hours. All bench surfaces and pipettes were treated with RNase AWAY decontamination reagent. All buffers used in the activity assays were freshly prepared with DEPC-treated water.

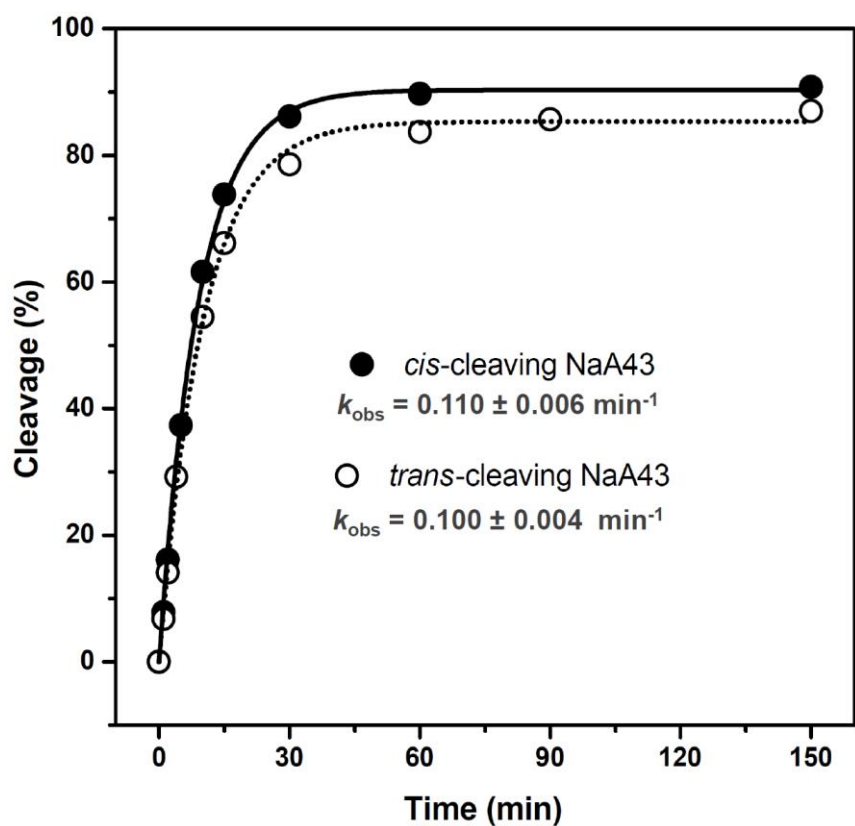


Figure S9. Activity assay results of *cis*-cleaving and *trans*-cleaving forms of the NaA43 DNAzyme in the presence of 400 mM NaCl showing little difference in the activity of the two forms.

Section S4. SI Figures for design and development of DNAzyme based sensors

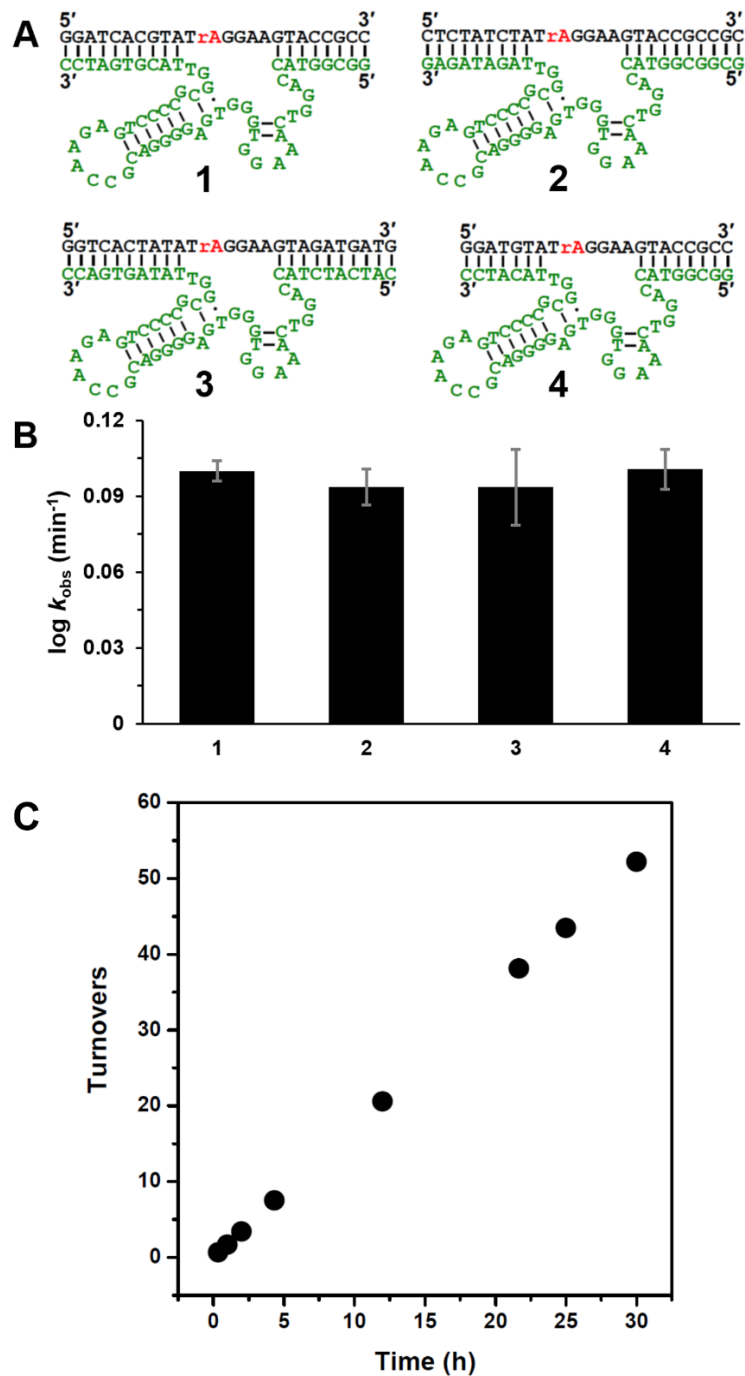


Figure S10. (A) NaA43 DNAzyme is represented with four different binding arms. (B) Activity of the four different versions of NaA43 DNAzyme was tested at 400 mM Na⁺ and k_{obs} values were obtained from at least two independent experiments. Error bars are represented by the standard deviation of the repeats performed. (C) Cleavage reaction under multiple-turnover condition in which NaA43S concentration was ~100 times higher than NaA43E. Assay was carried out using construct 1 in (A) with 50 mM NaCl at 22 °C.

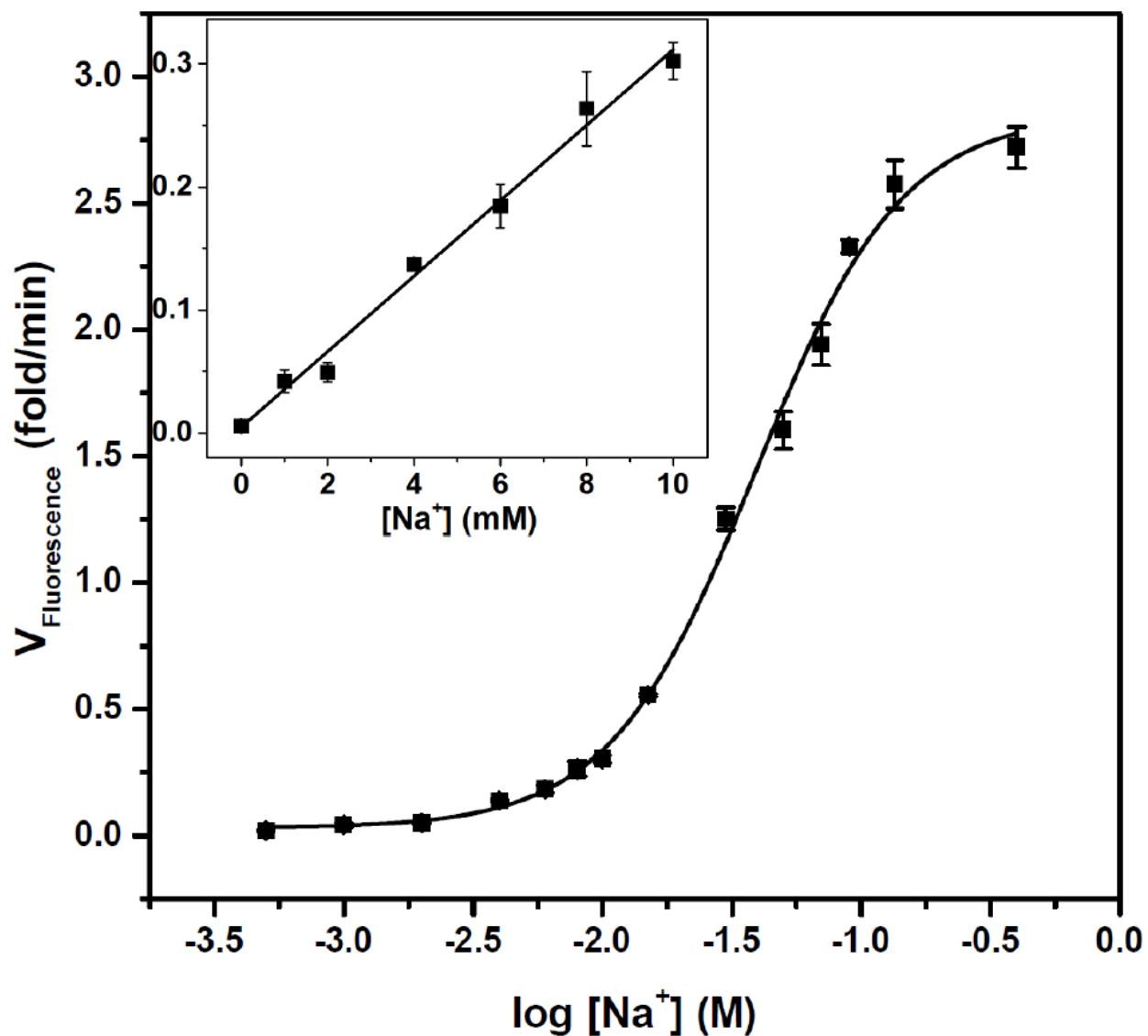


Figure S11. Rate of the initial fluorescence enhancement was calculated for different Na^+ concentration up to 400 mM. The change in the initial fluorescence enhancement leads to an apparent $K_d = 39.1 \pm 2.3$ mM. The apparent Hill coefficient was 1.5 ± 0.2 for the reaction in the presence of Li^+ . Inset represents linear response of the sensor at Na^+ concentrations lower than 10 mM. Error bars represent the standard deviation calculated from three independent experiments.

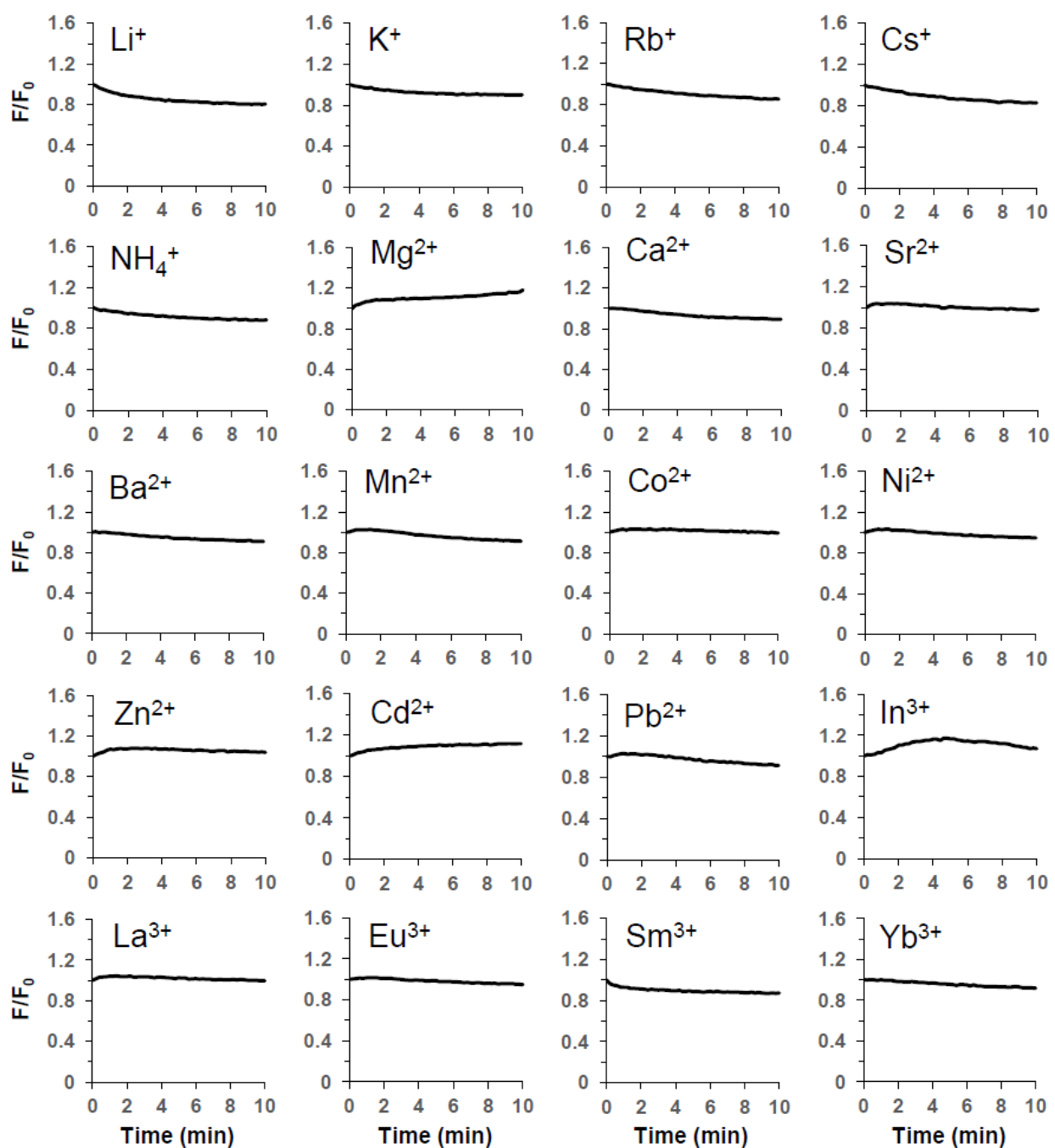


Figure S12. (A) Kinetic traces of NaA43 fluorescent sensor in response to metal ions other than sodium. Concentrations of metal ions were 100 mM, 2 mM and 0.2 mM for mono-, di-, and trivalent metal ions, respectively.

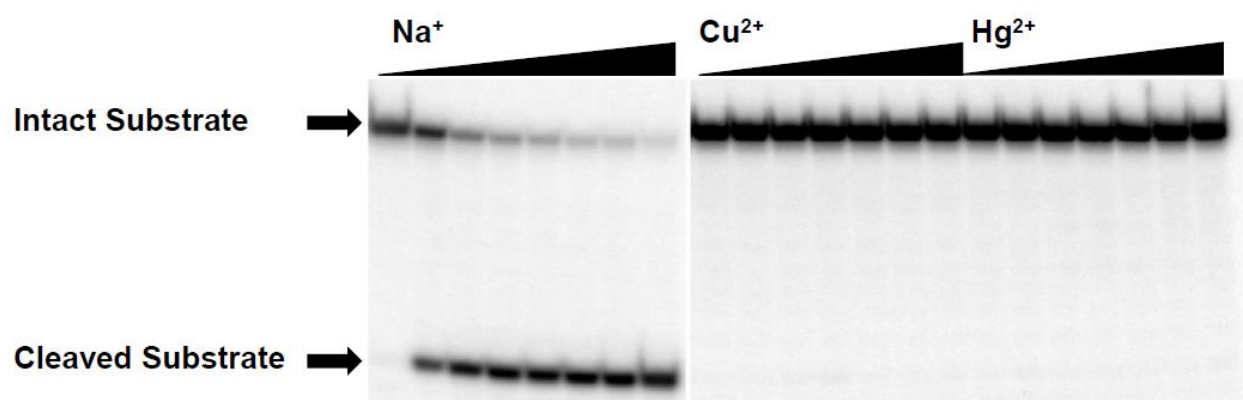


Figure S13. Selectivity of NaA43 was tested for Na^+ over Cu^{2+} and Hg^{2+} that induce a strong quenching on FAM using a gel-based cleavage assay with ^{32}P radiolabeled substrate in the presence of 2 mM Cu^{2+} and Hg^{2+} . In contrast to Na^+ , no cleavage was observed over 6 h course of the reaction in the presence of Cu^{2+} and Hg^{2+} . First lane of each set represents uncleaved substrate before addition of Na^+ . Uncleaved substrate and cleavage product (5' cleavage fragment) are marked by black arrows.

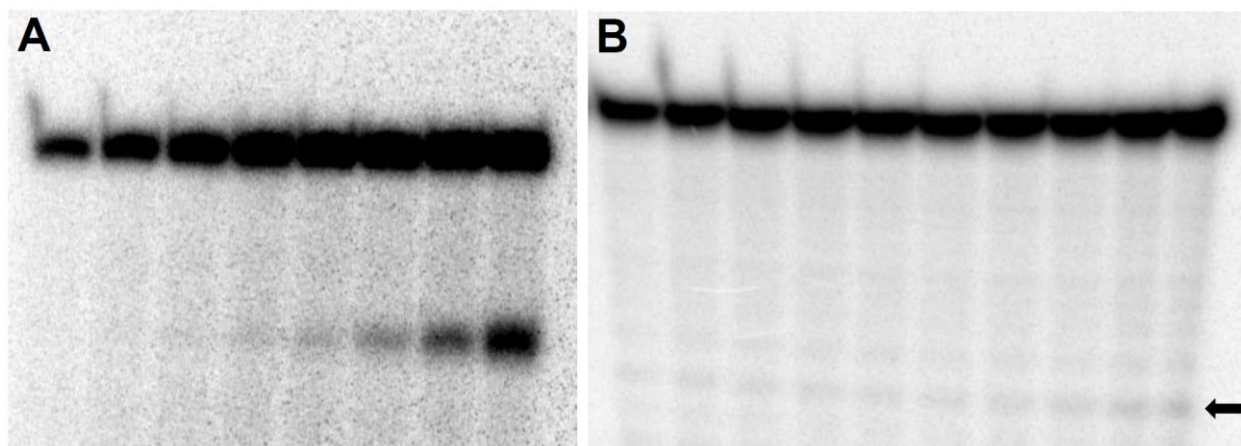


Figure S14. Activity of NaA43 was tested in the presence of 0.5 mM Na⁺ (A) and 5 M Li⁺ (B) over 25 h reaction time. Although 0.5 mM Na⁺ resulted in ~20% cleavage after 25 h (last lane in A), 5 M Li⁺ showed negligible cleavage over the same time period. Cleavage product (5' cleavage fragment) in B is marked by a black arrow.

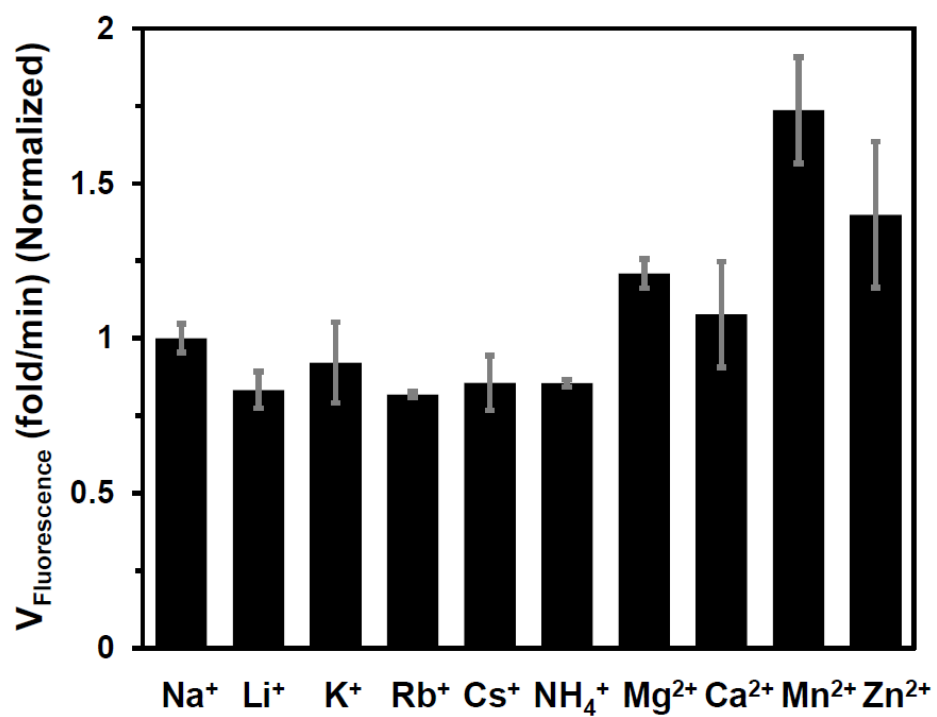


Figure S15. The rates of fluorescence increase of the NaA43 DNAzyme sensor in the presence of a mixture of 100 mM Na⁺ and either 100 mM Li⁺, Rb⁺, Cs⁺ or NH₄⁺, 140 mM K⁺, 0.5 mM Mg²⁺, 1 μM Ca²⁺, 100 μM Mn²⁺ or 100 μM Zn²⁺. Error bars are represented by the standard deviation of the repeats performed (at least two independent experiments).

Section S5. Figures for activity test of the intracellular sensor in buffer

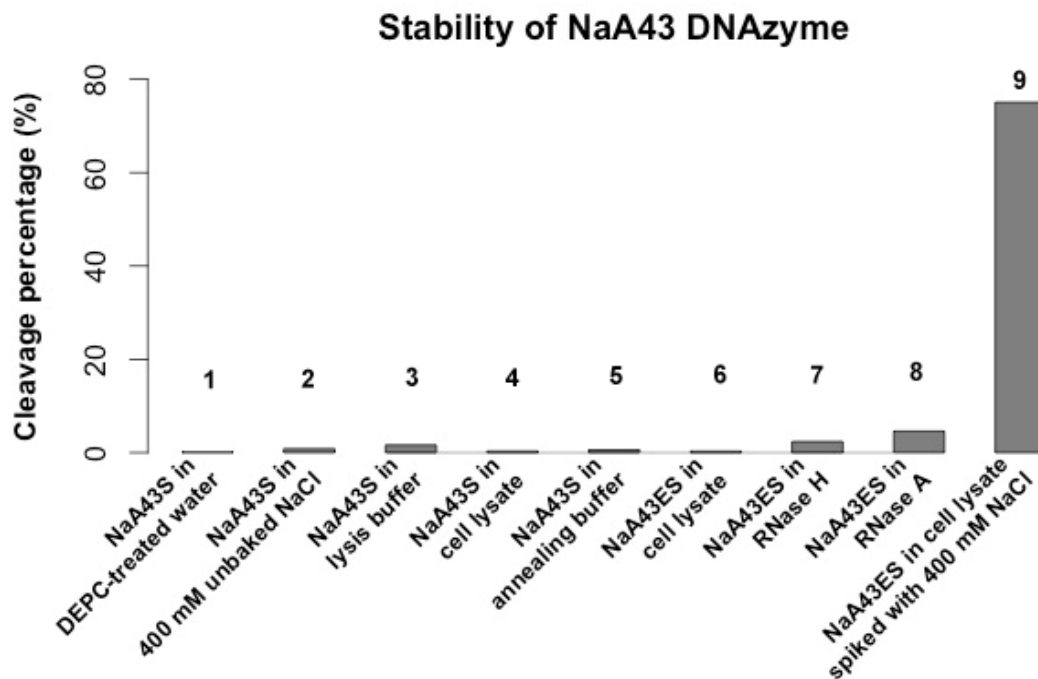


Figure S16. Stability of the NaA43 DNzyme. NaA43S or NaA43ES was incubated in the following conditions for 2 hours. NaA43S in (1) DEPC-treated water; (2) 400 mM unbaked NaCl; (3) lysis buffer containing 10 mM Tris-HCl (pH 7.5), 10 mM KCl, 1 mM EDTA, 0.1% Triton-X100, and 1× protease inhibitor cocktail (EDTA-free); (4) HeLa cell lysate; (5) annealing buffer containing 50 mM Bis-Tris (pH 7.0), 112 mM LiCl in DEPC-treated water; NaA43ES complex in (6) HeLa cell lysate; (7) 1 unit of RNase H (BioLabs); (8) 5 units of RNase A (Thermo Scientific); (9) HeLa cell lysate spiked with 400 mM NaCl.

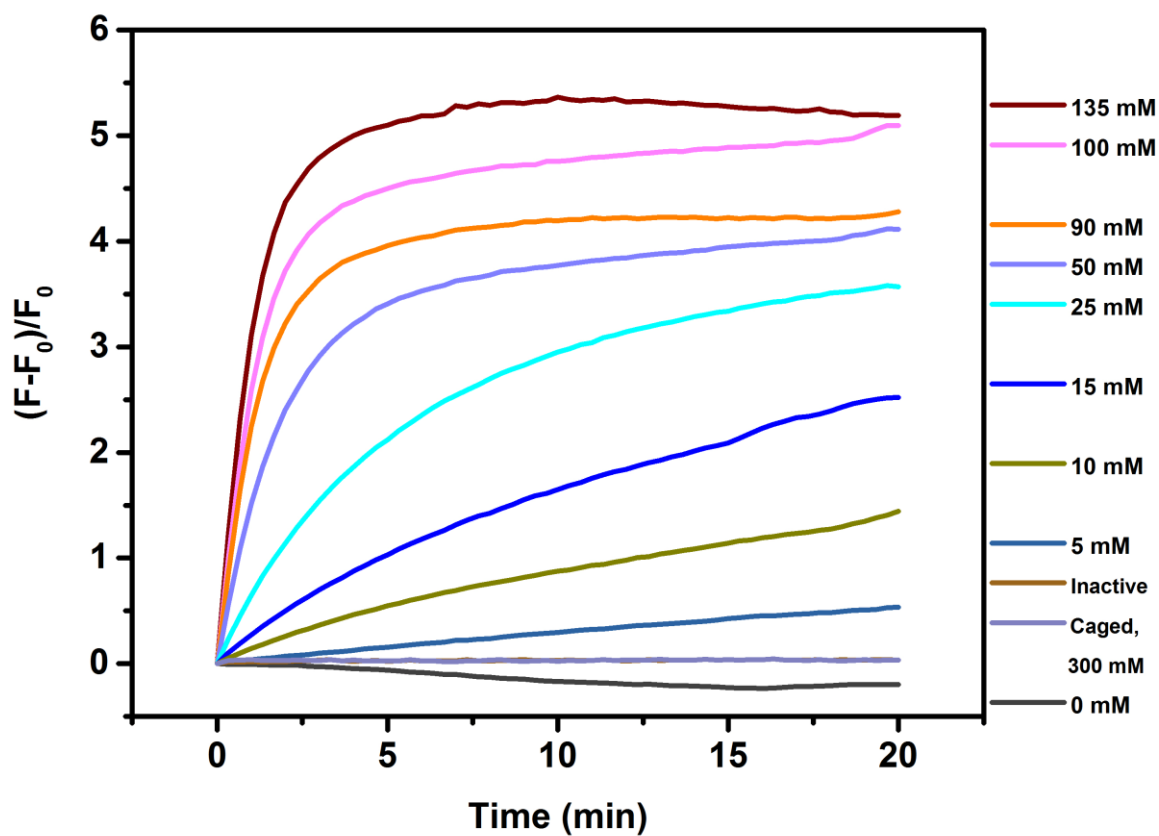


Figure S17. Turn-on fluorescence of NaA43ES sensor in buffer solution with different concentrations of Na⁺. Active Na43E (IBRQ) and Caged NaS (TAMRA-BHQ2) were used as the constructs of the sensor, and activity was measured after decaging the sensor at 365 nm for 30 min. In addition, the activity of an inactive mutant construct of NaA43ES (see sequence in S1 sequences, section 4.2.2) was tested, as well as the caged NaA43ES in the presence of 300 mM Na⁺. The activity of both the inactive mutant and caged NaA43ES overlapped and remained at the baseline over 20-minute reaction time.

Section S6. Figures for cell culture, sensor delivery and co-localization study

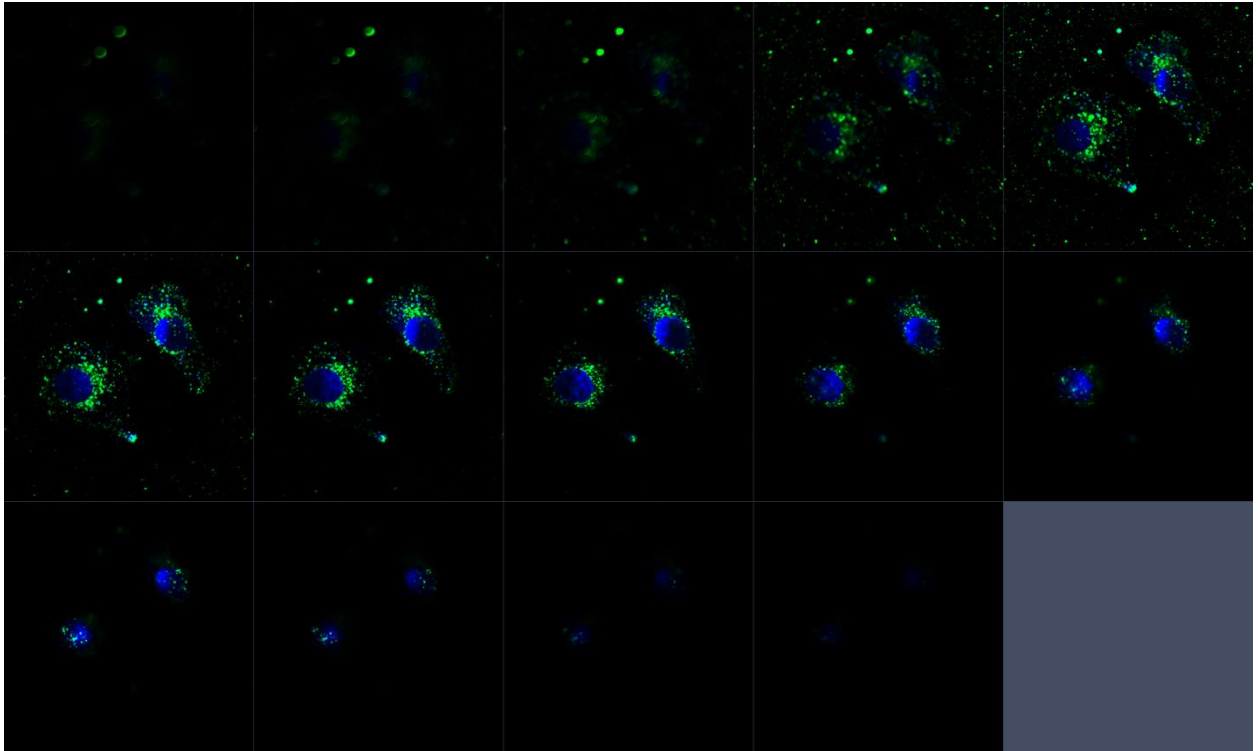


Figure S18. Z-stack images of HeLa cells with G8-NaA43ES complex. The green channel is FAM fluorescence from FAM-labeled non-cleavable NaA43S (FAM-dANa43S, see sequences SI Section S1, part 3). The blue channel is Hoechst 33258 for nucleus staining.

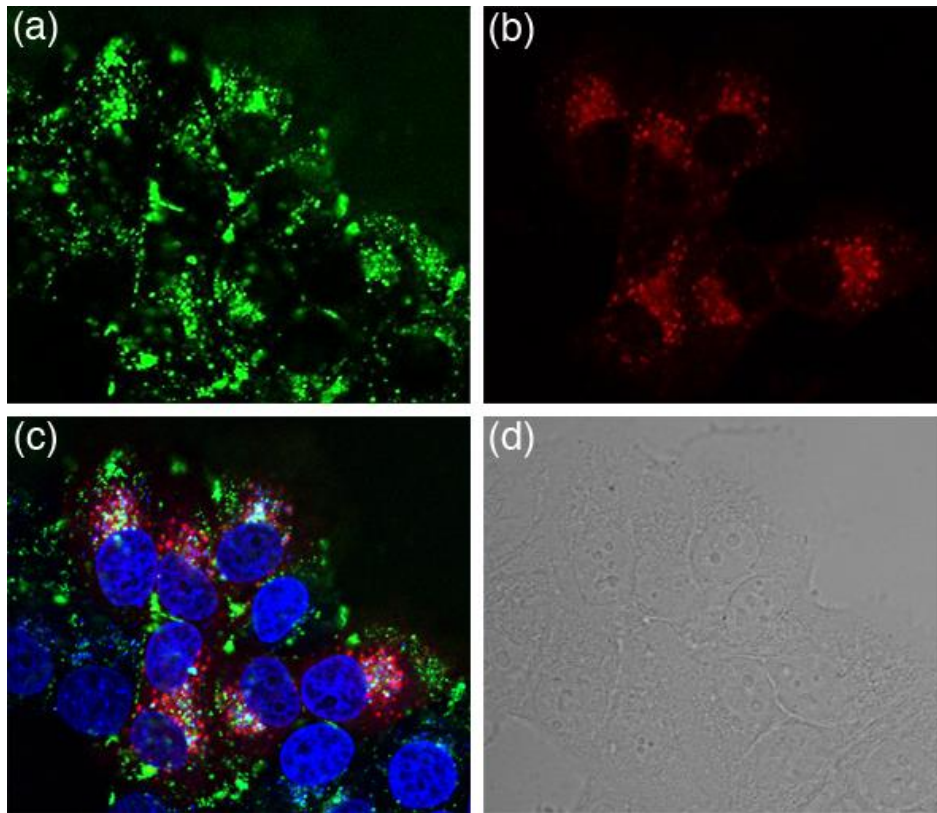


Figure S19. Co-localization of G8-NaA43 DNAzyme complex with early endosomes-RFP tracker. (a) green fluorescence from FAM-labeled NaA43 DNAzyme (see sequences in SI Section S1, part 3) delivered by G8 polypeptide; (b) red fluorescence from early endosomes-RFP expressed in the cells; (c) overlay of (a) and (b); (d) bright-field image of cells.

Section S7. Figures for live cell sodium sensing

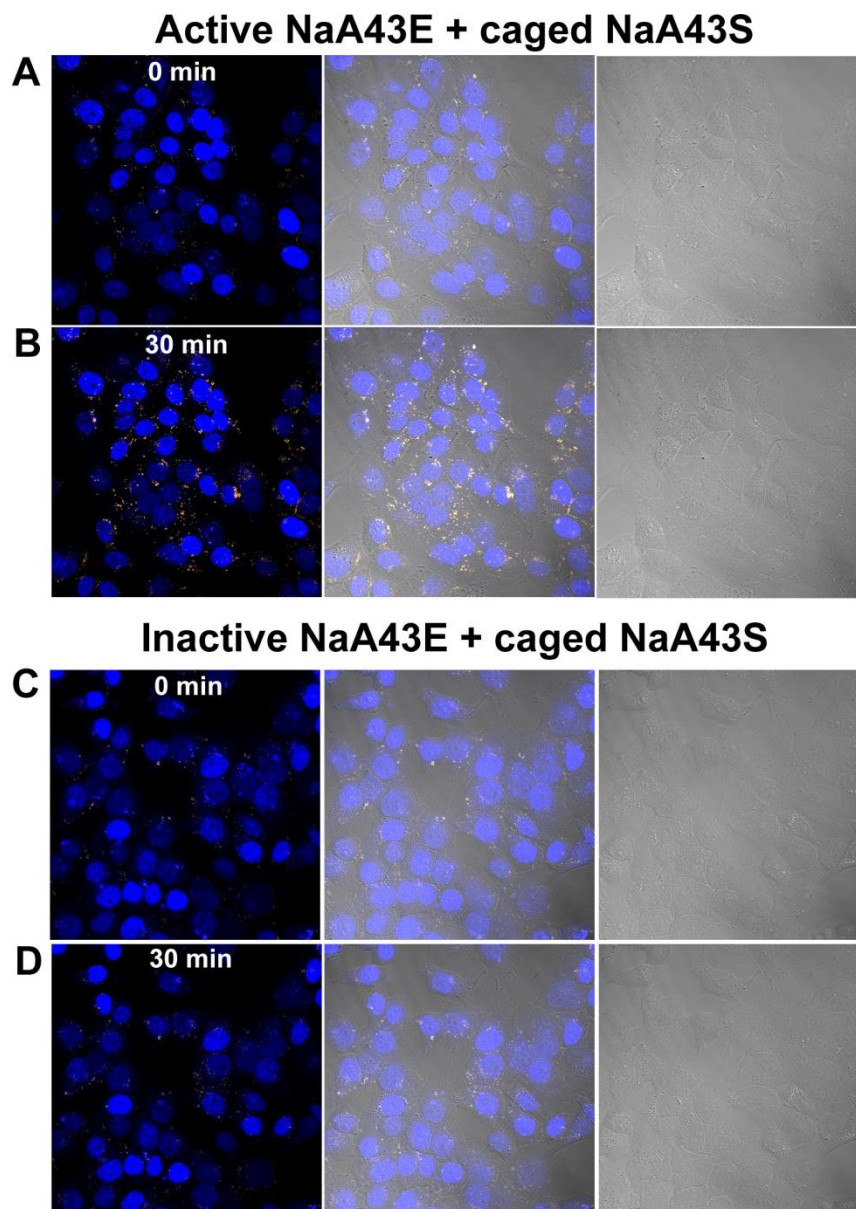


Figure S20. Confocal images of Na⁺ sensing using caged NaA43S (TAMRA-BHQ2) as the substrate. To confirm the activity of NaA43E after decaging process, an inactive NaA43E construct that contains a single-point mutation was used as the control group (see sequence in SI, Section S1, Sequences 4.2.2). (A, B) Fluorescent and bright field images of cells delivered with active NaA43E-IBRQ and caged NaA43S (TAMRA-BHQ2) construct. Images were taken (A) immediately after adding ionophores or (B) after 30 minutes. (C, D) Fluorescent and bright field images of cells delivered with inactive NaA43E (IBRQ) and caged NaA43S (TAMRA-BHQ2) construct. Images were taken (C) immediately after adding ionophores, or (D) after 30 minutes.

Class-III	B42- GTTCAGACTAATCATCACGATATAGGAATACCGCATGTTACAGTCAAAGGTTGGTTACAGGAACTTGTATAAATTCCTGTTG-GTTTCGTGAGCCTACGATGAGAC
	B48- GTTCAGACTAATCATCACGATATAGGAATACCGCATGTTACAGTCAAAGGTTGGTTGTCAGGAACTTGTATAAATTCCTGTTG-GTTTCGTGAGCCTACGATGAGAC
	B22- GTTCAGACTAATCATCACGATATAGGAATACCGCATGTTACAGTCAAAGGTTGGTTGTCAGGAACTTGTATAAATTCCTGTTG-GTTTCGTGAGCCTACGATGAGAC
	B36- GTTCAGACTAATCATCACGATATAGGAATACCGCATGTTACAGTCAAAGGTTGGTTGTCAGGAACTTGTATAAATTCCTGTTG-GTTTCGTGAGCCTACGATGAGAC
Class-II	B45- GTTCAGACTAATCATCACGATATAGGAATACCGCATGTTACCGGTTCAAAGGGG-SGTGT--TCACCTCGGTTCAACCTTAAGCTTAATGGTTACGTGAGCCTACGATGAGAC
	B49- GTTCAGACTAATCATCACGATATAGGAATACCGCATGTTACCGGTTCAAAGGGG-SGTGT--TCACCTCGGTTCAACCTTAAGCTTAATGGTTACGTGAGCCTACGATGAGAC
	B7- GTTCAGACTAATCATCACGATATAGGAATACCGCATGTTACCGGTTCAAAGGGG-SGTGT--TCACCTCGGTTCAACCTTAAGCTTAATGGTTACGTGAGCCTACGATGAGAC
	B9- GTTCAGACTAATCATCACGATATAGGAATACCGCATGTTACCGGTTCAAAGGGG-SGTGT--TCACCTCGGTTCAACCTTAAGCTTAATGGTTACGTGAGCCTACGATGAGAC
Orphan Orphan Duplet-I	B25- GTTCAGACTAATCATCACGATATAGGAATACCGCATGTTACCGGTTCAAAGGGG-SGTGT--TCACCTCGGTTCAACCTTAAGCTTAATGGTTACGTGAGCCTACGATGAGAC
	B47- GTTCAGACTAATCATCACGATATAGGAATACCGCATGTTACTTACCTCAAGAGGSCGAATCAATAAGCTATGCATGAAG--GGCTATTCGTGAGCCTACGATGAGAC
	B35- GTTCAGACTAATCATCACGATATAGGAATACCGCATGTTACTTACCTCAAGAGGSGG---ATCBAATACGGCTTCAGAACTAGGTAATACCSTGAGCCTACGATGAGAC
	B46- GTTCAGACTAATCATCACGATATAGGAATACCGCATGTTACCGGTTCAAAGGTTG-SGTG---TTTCATTTGATTCATTAATTAAGTGGTTACGTGAGCCTACGATGAGAC
	B38- GTTCAGACTAATCATCACGATATAGGAATACCGCATGTTACAGTCAAAGGTTG-SGTG---TTTCATTTGATTCATTAATTAAGTGGTTACGTGAGCCTACGATGAGAC
	B5- GTTCAGACTAATCATCACGATATAGGAATACCGCATGTTACTAGTCAAAGGTTGGTTT-TGGATCTTATAGAGAGATCCGAGATG-GTTACGTGAGCCTACGATGAGAC
	B23- GTTCAGACTAATCATCACGATATAGGAATACCGCATGTTACTAGTCAAAGGTTGGTTT-TGGATCTTATAGAGAGATCCGAGATG-GTTACGTGAGCCTACGATGAGAC
	B24- GTTCAGACTAATCATCACGATATAGGAATACCGCATGTTACTAGTCAAAGGTTGGTTT-TGGATCTTATAGAGAGATCCGAGATG-GTTACGTGAGCCTACGATGAGAC
	B15- GTTCAGACTAATCATCACGATATAGGAATACCGCATGTTACCGGGTACGGGACCGCTG-TCAAACCGATACCGGTTAAGTTG-GTTTCGTGAGCCTACGATGAGAC
	B33- GTTCAGACTAATCATCACGATATAGGAATACCGCATGTTACCGGGTACGGGACCGCTG-TCAAACCGATACCGGTTAAGTTG-GTTTCGTGAGCCTACGATGAGAC
Class-I	B4- GTTCAGACTAATCATCACGATATAGGAATACCGCATGTTACCGGTTCAAAGGTTG-SGTG---AGGGGACGCCAAGAGTCCCCGCGGTTACGTGAGSTGAGCCTACGATGAGAC
	B12- GTTCAGACTAATCATCACGATATAGGAATACCGCATGTTACCGGTTCAAAGGTTG-SGTG---AGGGGACGCCAAGAGTCCCCGCGGTTACGTGAGSTGAGCCTACGATGAGAC
	B11- GTTCAGACTAATCATCACGATATAGGAATACCGCATGTTACCGGTTCAAAGGTTG-SGTG---AGGGGACGCCAAGAGTCCCCGCGGTTACGTGAGSTGAGCCTACGATGAGAC
	B21- GTTCAGACTAATCATCACGATATAGGAATACCGCATGTTACCGGTTCAAAGGTTG-SGTG---AGGGGACGCCAAGAGTCCCCGCGGTTACGTGAGSTGAGCCTACGATGAGAC
	B3- GTTCAGACTAATCATCACGATATAGGAATACCGCATGTTACTAGTCAAAGGTTGGTTG---AGGGGACGCCAAGAGTCCCCGCGGTTACGTGAGSTGAGCCTACGATGAGAC
	B31- GTTCAGACTAATCATCACGATATAGGAATACCGCATGTTACTAGTCAAAGGTTGGTTG---AGGGGACGCCAAGAGTCCCCGCGGTTACGTGAGSTGAGCCTACGATGAGAC
	B19- GTTCAGACTAATCATCACGATATAGGAATACCGCATGTTACTAGTCAAAGGTTGGTTG---AGGGGACGCCAAGAGTCCCCGCGGTTACGTGAGSTGAGCCTACGATGAGAC
	B13- GTTCAGACTAATCATCACGATATAGGAATACCGCATGTTACTAGTCAAAGGTTGGTTG---AGGGGACGCCAAGAGTCCCCGCGGTTACGTGAGSTGAGCCTACGATGAGAC
	B30- GTTCAGACTAATCATCACGATATAGGAATACCGCATGTTACTAGTCAAAGGTTGGTTG---AGGGGACGCCAAGAGTCCCCGCGGTTACGTGAGSTGAGCCTACGATGAGAC
	B40- GTTCAGACTAATCATCACGATATAGGAATACCGCATGTTACTAGTCAAAGGTTGGTTG---AGGGGACGCCAAGAGTCCCCGCGGTTACGTGAGSTGAGCCTACGATGAGAC
	B17- GTTCAGACTAATCATCACGATATAGGAATACCGCATGTTACTAGTCAAAGGTTGGTTG---AGGGGACGCCAAGAGTCCCCGCGGTTACGTGAGSTGAGCCTACGATGAGAC
	B27- GTTCAGACTAATCATCACGATATAGGAATACCGCATGTTACTAGTCAAAGGTTGGTTG---AGGGGACGCCAAGAGTCCCCGCGGTTACGTGAGSTGAGCCTACGATGAGAC
	B6- GTTCAGACTAATCATCACGATATAGGAATACCGCATGTTACTAGTCAAAGGTTGGTTG---AGGGGACGCCAAGAGTCCCCGCGGTTACGTGAGSTGAGCCTACGATGAGAC
	B10- GTTCAGACTAATCATCACGATATAGGAATACCGCATGTTACTAGTCAAAGGTTGGTTG---AGGGGACGCCAAGAGTCCCCGCGGTTACGTGAGSTGAGCCTACGATGAGAC
	B43- GTTCAGACTAATCATCACGATATAGGAATACCGCATGTTACTAGTCAAAGGTTGGTTG---AGGGGACGCCAAGAGTCCCCGCGGTTACGTGAGSTGAGCCTACGATGAGAC
	B44- GTTCAGACTAATCATCACGATATAGGAATACCGCATGTTACTAGTCAAAGGTTGGTTG---AGGGGACGCCAAGAGTCCCCGCGGTTACGTGAGSTGAGCCTACGATGAGAC
	B2- GTTCAGACTAATCATCACGATATAGGAATACCGCATGTTACTAGTCAAAGGTTGGTTG---AGGGGACGCCAAGAGTCCCCGCGGTTACGTGAGSTGAGCCTACGATGAGAC
	B16- GTTCAGACTAATCATCACGATATAGGAATACCGCATGTTACTAGTCAAAGGTTGGTTG---AGGGGACGCCAAGAGTCCCCGCGGTTACGTGAGSTGAGCCTACGATGAGAC
	B18- GTTCAGACTAATCATCACGATATAGGAATACCGCATGTTACTAGTCAAAGGTTGGTTG---AGGGGACGCCAAGAGTCCCCGCGGTTACGTGAGSTGAGCCTACGATGAGAC
	B20- GTTCAGACTAATCATCACGATATAGGAATACCGCATGTTACTAGTCAAAGGTTGGTTG---AGGGGACGCCAAGAGTCCCCGCGGTTACGTGAGSTGAGCCTACGATGAGAC
	B26- GTTCAGACTAATCATCACGATATAGGAATACCGCATGTTACTAGTCAAAGGTTGGTTG---AGGGGACGCCAAGAGTCCCCGCGGTTACGTGAGSTGAGCCTACGATGAGAC
	B34- GTTCAGACTAATCATCACGATATAGGAATACCGCATGTTACTAGTCAAAGGTTGGTTG---AGGGGACGCCAAGAGTCCCCGCGGTTACGTGAGSTGAGCCTACGATGAGAC
	B41- GTTCAGACTAATCATCACGATATAGGAATACCGCATGTTACTAGTCAAAGGTTGGTTG---AGGGGACGCCAAGAGTCCCCGCGGTTACGTGAGSTGAGCCTACGATGAGAC
	B29- GTTCAGACTAATCATCACGATATAGGAATACCGCATGTTACTAGTCAAAGGTTGGTTG---AGGGGACGCCAAGAGTCCCCGCGGTTACGTGAGSTGAGCCTACGATGAGAC
	B50- GTTCAGACTAATCATCACGATATAGGAATACCGCATGTTACTAGTCAAAGGTTGGTTG---AGGGGACGCCAAGAGTCCCCGCGGTTACGTGAGSTGAGCCTACGATGAGAC
	B8- GTTCAGACTAATCATCACGATATAGGAATACCGCATGTTACTAGTCAAAGGTTGGTTG---AGGGGACGCCAAGAGTCCCCGCGGTTACGTGAGSTGAGCCTACGATGAGAC
	B14- GTTCAGACTAATCATCACGATATAGGAATACCGCATGTTACTAGTCAAAGGTTGGTTG---AGGGGACGCCAAGAGTCCCCGCGGTTACGTGAGSTGAGCCTACGATGAGAC
	B28- GTTCAGACTAATCATCACGATATAGGAATACCGCATGTTACTAGTCAAAGGTTGGTTG---AGGGGACGCCAAGAGTCCCCGCGGTTACGTGAGSTGAGCCTACGATGAGAC

Table S2. 48 individual clones resulting from sequencing the selected pool from selection B. Sequence alignment was carried out by Vector NTI. Obtained sequences from Selection B fall into three major classes and the majority of them belong to class I.

Section S9. SI References

1. Breaker RR & Joyce GF (1994) A DNA enzyme that cleaves RNA. *Chem Biol* 1(4):223-229.
2. Santoro SW & Joyce GF (1997) A general purpose RNA-cleaving DNA enzyme. *Proc Natl Acad Sci U S A* 94(9):4262-4266.
3. Li J, Zheng W, Kwon AH, & Lu Y (2000) In vitro selection and characterization of a highly efficient Zn(II)-dependent RNA-cleaving deoxyribozyme. *Nucleic Acids Res* 28(2):481-488.
4. Markham NR & Zuker M (2005) DINAMelt web server for nucleic acid melting prediction. *Nucleic Acids Res* 33(Web Server issue):W577-581.
5. Markham NR & Zuker M (2008) UNAFold: software for nucleic acid folding and hybridization. *Methods Mol Biol* 453:3-31.
6. Murray JB, Seyhan AA, Walter NG, Burke JM, & Scott WG (1998) The hammerhead, hairpin and VS ribozymes are catalytically proficient in monovalent cations alone. *Chem Biol* 5(10):587-595.
7. Joyce GF (2004) Directed evolution of nucleic acid enzymes. *Annu Rev Biochem* 73:791-836.
8. Liu J, *et al.* (2007) A catalytic beacon sensor for uranium with parts-per-trillion sensitivity and millionfold selectivity. *Proc Natl Acad Sci U S A* 104(7):2056-2061.
9. Bruesehoff PJ, Li J, Augustine AJ, 3rd, & Lu Y (2002) Improving metal ion specificity during in vitro selection of catalytic DNA. *Comb Chem High Throughput Screen* 5(4):327-335.
10. Stage-Zimmermann TK & Uhlenbeck OC (1998) Hammerhead ribozyme kinetics. *RNA* 4(8):875-889.